Journal of Climate Change Research 2017, Vol. 8, No. 4, pp. 287~295
DOI: http://dx.doi.org/10.15531/KSCCR.2017.8.4.287

Flood Risk for Power Plant using the Hydraulic Model and Adaptation Strategy

Nguyen, Thanh Tuu[*], Kim, Seungdo[*†], Van, Pham Dang Tri[**], Lim, Jeejae[*], Yoo, Beomsik[*] and Kim, Hyeonkyeong[***]

[*]*Dept. of Environmental Science and Biotechnology, College of Natural Sciences, Hallym University, Korea*
[**]*Dept. of Water Resources, College of Environment and Natural Resources, Can Tho University, Vietnam*
[***]*Division of Information and Telecommunications, Hanshin University, South Korea*

ABSTRACT

This paper provides a mathematical approach for estimating flood risks due to the effects of climate change by developing a one dimensional (1D) hydraulic model for the mountainous river reaches located close to the Yeongwol thermal power plant. Input data for the model, including topographical data and river discharges measured every 10 minutes from July 1st to September 30th, 2013, were imported to a 1D hydraulic model. Climate change scenarios were estimated by referencing the climate change adaptation strategies of the government and historical information about the extreme flood event in 2006. The down stream boundary was determined as the friction slope, which is 0.001. The roughness coefficient of the main channels was determined to be 0.036. The results show the effectiveness of the riverbed widening strategy through the six flooding scenarios to reduce flood depth and flow velocity that impact on the power plant. In addition, the impact of upper Namhan River flow is more significant than Dong River.

Key words: *1D Hydraulic Model, Thermal Power Plant, Climate Change, Risk Prediction*

1. INTRODUCTION

Climate change is a global concern because of much more extreme disaster events in the recent year (Anderson and Bausch, 2006). One of the key impacts of climate change could be an extreme flood event caused by major storms and heavy rainfall (Bilskie *et al.*, 2016; Easterling *et al.*, 2000). The probability of flood events was estimated to become higher in the future due to climate change (de Bruijn *et al.*, 2017; Jonkman and Vrijling, 2008; Mohleji, 2011; Monirul Qader Mirza, 2002).

The Han River Basin is located in the North East of South Korea with the high mountain region, the largest basin of the country as well as Korea Peninsula, and is spread over four provinces, including Gangwon-do, Gyeonggi-do, Seoul and Chungcheongbuk-do. The annual average precipitation is approximately 1,200 mm during 1961~1990 (Jeong *et al.*, 2005; Jung *et al.*, 2001), and the rainy season occurs from June to September. Han River Basin can be divided into three sub-basin, including Han, Bukhan and Namhan Sub-basin. Yeongwol City is located in the East of Namhan Sub-basin (Fig. 1). Under the impact of climate change, the rainy days tend to decrease and the storms become heavier. The heavy rainfall

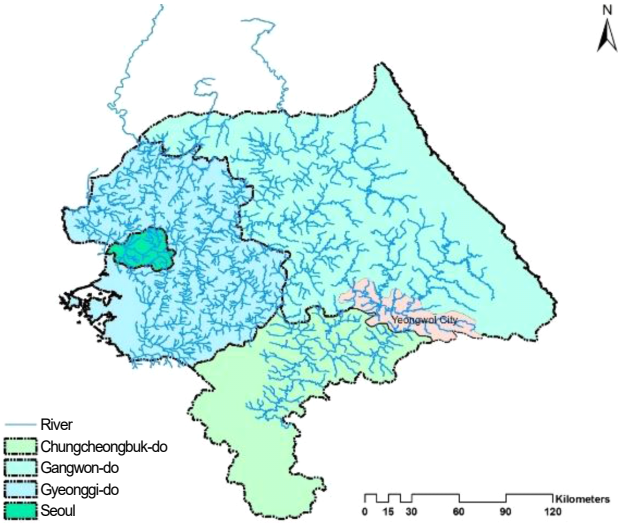

Fig. 1. Han River basin.

† **Corresponding author:** sdkim@hallym.ac.kr
Received October 16, 2017 / Revised November 13, 2017 1st, November 24, 2017 2nd / Accepted December 2, 2017
* Pictures are shown in color version online.

increased from about 100 mm to 222 mm in 1971 and 1980; and, 325 mm in 1992 and 2001 (WWAP, 2009).

Many hydrological models were developed to analyze the climate change impacts on water resources and land use in different basins, including Chungju Basin (Bae *et al.*, 2011) and Hoeya River Basin (Kim *et al.*, 2013). It was found that the trend of water discharges in the river increase in the wet periods and decrease in the dry periods. However, the flood risk prediction in the sub-basin in Yeongwol City was not yet implemented. In Gangwon Province, the rainy season with an extremely high precipitation caused extreme flood event in the summer in 2006 (Chang *et al.*, 2009; Na *et al.*, 2012). According to the data collected from Han River Flood Control Office (HRFCO), in the major flood event in July 2006, the peak water level was 11 m in the main channel at Yeongwol Bridge on Dong River.

In this study, a one dimensional hydraulic model was developed for simulating the dynamics of a small reach of Namhan River and Dong River located in Yeongwol City. Moreover, the flood depths were simulatedby running the model with different scenarios, provided that the upstream urbanarea is protected by full-dyke system.

2. METHODOLOGY

2.1 Model Development

The model was developed in Step 1, and the calibrated and validated in Step 2. The first step includes: (1) obtaining and analyzing the 90 m resolution DEM as map format; (2) converting to geometric data by using HEC-GeoRAS tool; and, (3) importing the boundary conditions to HEC-RAS. The model was then calibrated and validated to make sure it was applicable (Step 2). In this step, there is 4 main sub-steps including: (1) calculation of Nash-Sutcliffe (NS) values after calibration; (2) validation in a different year; (3) calculation of NS values after validation; and, (4) finishing the model if NS values meet the highest value ($0.75 \ll NS \leq 1$). If NS values are lower than 0.75, there will be 4 extra steps, including: (3'), (4'), (5') and (6'). Then it is calibrated again until NS meet the highest value (Fig. 2).

This model is a tool for assessing the impact of climate change on the power plant, especially flood events. The applicable model can be used to predict the impacts of climate change under the future scenarios.

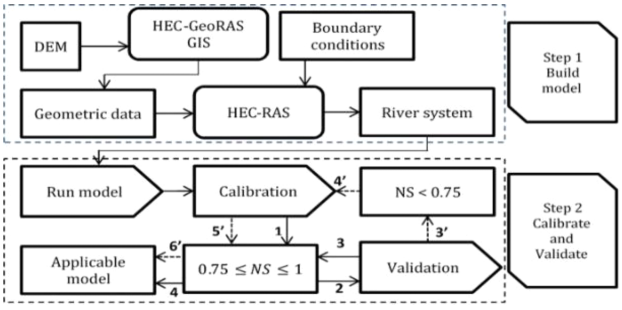

Fig. 2. Steps of model development.

2.2 Model Description

DEM of the study region: The 90 m resolution digital elevation model (DEM) was collected from the Consultative Group on International Agriculture Research-Consortium for Spatial Information (available at www.cgiar-csi.org). The DEM of South Korea was obtained to creating geometric data and focused on Yeongwol district, Gangwon Province, which is located near the power plant (Fig. 3). The DEM was used for cross section interpolation, and the cross-sections are then imported to HEC-RAS program to develop the model.

Geometric data: The main geometric data included stream centerlines (the line between two river banks); river cross-sec-

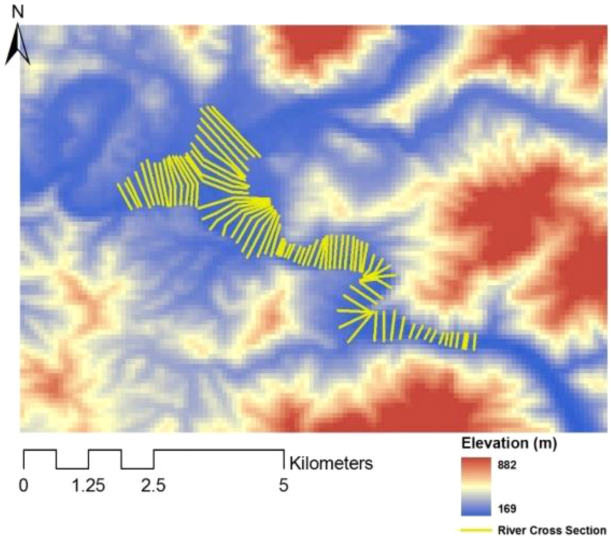

Fig. 3. Digital elevation model of study area.

tions, created from DEM by using HEC-GeoRAS in combination with GIS program; and, Manning's n roughness coefficients. The cross-sections were created based on the conditions: (a) the change of channel slopes; (b) the change of river widths; and, (c) the change of curves of the channel. The total length of the Namhan River reach in this study area was approximately 8,000 m (Fig. 4).

Boundary conditions: There are two upstream inputs, including flow rates in Yeongwol Bridge, located on Dong River, and Palgoe Bridge, located on Namhan River (Fig. 4). The flow rates ($m^3 \cdot s^{-1}$) were measured every 10 minutes and published on HRFCO (availableat www.hrfco.go.kr).

The downstream boundary, which is friction slope, is estimated by using the energy equation (Eq. (1)) (Chow *et al.*, 1988) as

$$Z_2 + Y_2 + V_2^2 / 2g = Z_1 + Y_1 + V_1^2 / 2g + h_e \quad (1)$$

where $Z_1$and Z_2: elevations of the main channel inverts (m); Y_1 and Y_2: water depths of downstream and upstream (m), respectively; V_1 and V_2: average velocities of downstream and upstream ($m \cdot s^{-1}$),respectively;: gravitational acceleration ($m \cdot s^{-2}$); and, h_e: energy head loss (m). The representation of terms of energy equation for open channel flow is shown in Fig. 5.

The friction slope (Canestrelli *et al.*, 2014; Cheikh, 2015; Wu *et al.*, 2015) is calculated by Eq. (2).

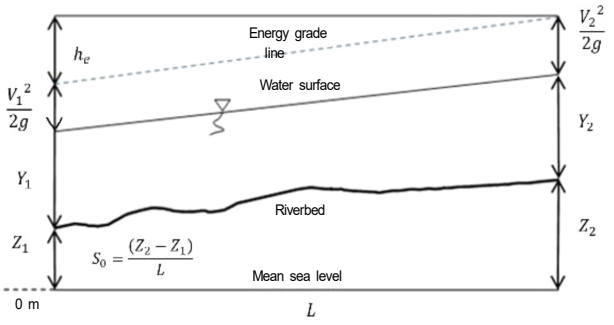

Fig. 5. Representation of terms in the equation for open channels.

$$S_f = \frac{h_e}{L} \quad (2)$$

where S_f: fiction slope; and, L: channel length (m).

The friction slope and channel slope have the same value ($S_0 = S_f$) in case of unsteady uniform flow (Chow *et al.*, 1988). Applied for the model, the friction slope can be estimated as Eq. (3). Then the value was used as downstream boundary input data.

$$S_0 = S_f = \frac{(Z_2 - Z_1)}{L} \quad (3)$$

where S_0: channel slope.

In this model, the estimated total length from upstream to

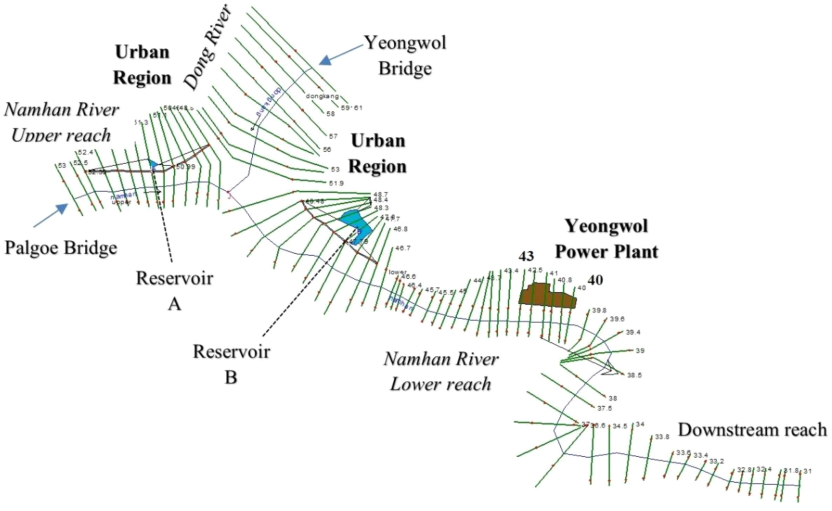

Fig. 4. Geometric data in the model.

downstream reaches is L = 8,000 m. The upstream elevation is Z_2 = 188 m, and the downstream elevation is Z_1 = 176 m. Therefore, the friction slope is calculated as S_f = 0.001 and used as the downstream boundary condition.

Manning's n roughness coefficients is the value indicating the flow obstacle in the rivers. There are many n values depending on different types of channel. The n values are limited between 0.012 and 0.100 for the main channel of natural streams (Alegre *et al.*, 2017; Bilskie *et al.*, 2016; Brunner, 2010; Chow *et al.*, 1988; Savage *et al.*, 2016). Manning's n equation is important for hydraulic study, it indicates the relation between flow rate, water level, n coefficient and friction slope (Eq. (4) and Eq. (5)).

$$Q = \frac{1}{n} \cdot A \cdot R^{\frac{2}{3}} \sqrt{S_f} \tag{4}$$

$$R = \frac{A}{P} \tag{5}$$

where Q: flow rate ($m^3 \cdot s^{-1}$); n: Manning's n roughness coefficient; A: flow area (m^2); R: hydraulic radius (m); and, P: wetted perimeter (m).

Model running: The year 2013 was chosen for running the model because there was a peak water depth of the period between 2009 and 2014, and the data of two upstream boundary conditions are sufficient. At Yeongwol Bridge Station, the maximum water level is 7.14 m on July 15th, and the maximum flow rate is approximately 7,000 $m^3 \cdot s^{-1}$. At Palgoe Bridge Station, the maximum water level is 9.40 m, and the maximum flow rate was nearly 5,700 $m^3 \cdot s^{-1}$.

2.3 Calibration and Validation

J. E. Nash and J.V. Sutcliffe created one index called Nash-Sutcliffe index (NS) that represents the accuracy of hydrological and hydraulic models (Habert *et al.*, 2016; Nash and Sutcliffe, 1970). Harmel *et al.* (2010) developed a watershed model was calibrated by using NS index, and it shows that the NS values are greater than 0.90 resulting in a good applied model ($0.75 \ll NS \leq 1$) (Moriasi and Arnold, 2007). The NS index was also used to calibrate the hydraulic model. For example, Panda *et al.* (2010) and Paiva *et al.* (2011) used NS to calibrate the hydraulic model for river networks. Besides, there were various studies using NS for comparing the simulated and observed water levels and discharge in 1D hydraulic model recently (de Paes and Brandão, 2013; Lotsari *et al.*, 2014; Meert *et al.*, 2016; Saleh *et al.*, 2013).

The NS value is calculated in Eq. (6). If the NS closes to one (100%), the model will be acceptable and can be applied.

$$\mathrm{NS} = 1 - \frac{\Sigma_1^m (X_{sim,i} - X_{obs,i})^2}{\Sigma_1^m (X_{obs,i} - \overline{X}_{obs})^2} \tag{6}$$

where NS: Nash-Sutcliffe Index; $X_{sim,i}$: simulated value at the time i; $X_{obs,i}$: observed value at the time i; $\overline{X}_{obs}$: average observed value in the period of calibration; m: number of hours.

In this case, X value represents the water level of the channel. Therefore, $X_{sim,i}$, $X_{obs,i}$, and $\overline{X}_{obs}$ were simulated, observed, and average observed water levels, respectively. In addition, the output data was simulated hourly and decided as 2,208 hours, from July 1st to September 30th, and that means m = 2,208.

The Manning's n roughness coefficients of the main channel were adjusted to make the simulated water levels closed to observed values. The model was tested with different n coefficients in a range from 0.012 to 0.100, and it would be stopped if the NS index met the highest values.

After calibration, the model was validated by running in the different periods, i.e. 2011, 2012 and 2014, to make sure that it is reasonable for other years. If the NS values were much lower than one, the n values would be adjusted again until it was applicable. The model was then computed in the first period, i.e. the year 2013, to make it applicable (Fig. 2).

Table 1 shows the Nash-Sutcliffe index of two upstream stations under calibration and validation. The results indicated that the NS values were very high, and it can be apply for simulation and prediction. Moreover, it was found that the Manning's n coefficient in the main channel of Namhan River and Dong River was 0.036, and it was used for all river cross

Table 1. NS index after calibration and validation

NS index	2011	2012	2013	2014
Yeongwol bridge	0.99	0.96	0.99	0.99
Palgoe bridge	0.98	0.99	0.99	0.96

sections.

The comparisons of water levels in the two upstream stations are shown in Fig. 6(a) and Fig. 6(b), and explained for the accuracy of the model (NS index). The periods of the highest water level was chosen to compare. The peak water level usually occurred in the period from 2nd to 16th of July in 2011 and 2013. Moreover, the simulated water levels almost equal to the observed values. The maximum water levels in 2012 and 2014 were quite low compared to the other years. The maximum observed and simulated water levels were 3.57 m and 3.54 m in 2012; and 2.47 m and 2.34 m in 2014, respectively.

2.4 Future Scenarios

The comparison of the discharges shows that the flood events in 2006 and the highest water level in 2013 occurred in the same period, i.e. the period from July 15th to July 17th,

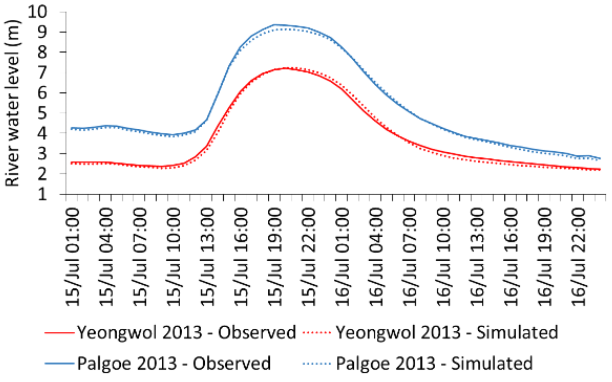

(a) 2011

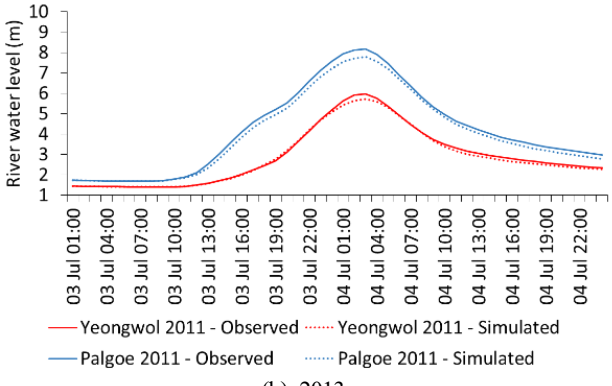

(b) 2013

Fig. 6. Simulated and observed water levels at Yeongwol and Palgoe Bridge Stations in 2011 and 2013.

at Yeongwol Bridge Station. The scenarios were determined based on the extreme flood event in 2006 and strategies to resist these problems. The maximum discharge in 2006 (about 19,000 $m^3 \cdot s^{-1}$) was approximately three times greater than that in 2013, which was nearly 6,000 $m^3 \cdot s^{-1}$.

The data of discharges and water levels at Yeongwol Bridge Station in 2006 is sufficient; however, the hydrodynamic data at Palgoe Bridge station in 2006 is missing. It was assumed that the future discharges at Yeongwol Bridge Station are three times greater than the flow in 2013 (Extremely High Flow). In addition, it was assumed that there will be three conditions for Palgoe Bridge Station in the future including: (1) the future flow equals to the flow in 2013 (Low Flow); (2) the future flow is double the flow in 2013 (High Flow); and, (3) the future flow is triple the flow in 2013 (Extremely High Flow). According to the data collected from HRFCO, a riverbed expansion strategy was decided in order to prevent the impact of flood event. The cross sections of the rivers were expanded to the maximum width and depth but the stable flow was still ensured. In this case, the average expanded depth is approximately 4 m, such as cross sections 48.7 and 31 [Fig. 4, Fig. 7(a) and 7(b)].

There are six scenarios based on the combination between future climate change conditions and the adaptation strategy (Table 2).

3. RESULTS AND DISCUSSION

3.1 Water Surface Elevations

According to the survey, the minimum ground surface elevation of the power plant is approximately 197 m, two-meter higher than the elevation of the road elevation (195 m). The cross section 42.5, located near the power plant, was chosen to analyze. Fig. 8 shows the simulated maximum water surface elevations from 2011 to 2014. The lowest elevation is in 2014 (black line) and the highest is in 2013 (yellow line). The historical maximum water elevations are below the bank station (road). The highest elevation in 2013 is approximately 193.3 m, and the lowest elevation in 2014 is 186.9 m. The depths in 2011 and 2012 are 191.7 m and 189.3 m, respectively. The maximum velocity is ranged from 1.8 $m \cdot s^{-1}$ (2014) to

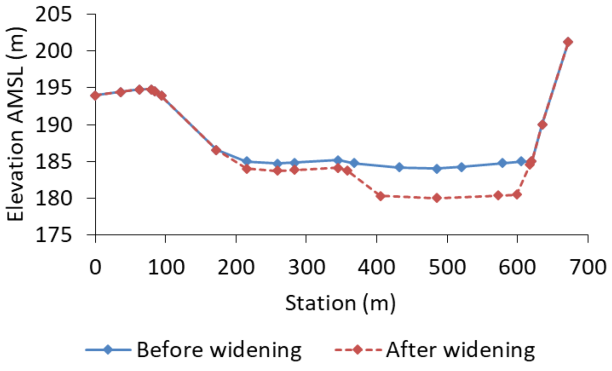

(a) Cross section 48.7

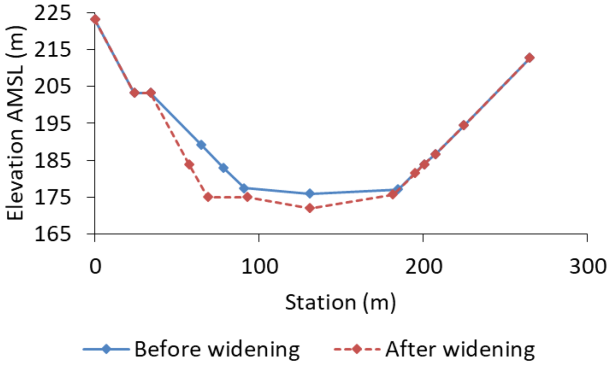

(b) Cross section 31

Fig. 7. Cross section data before and after widening at the upstream and downstream of the lower reach of Namhan River (AMSL: above mean sea level).

Table 2. Future scenario description

Scenario	Strategy	Upper Namhan flow	Dong River flow
Sce. 1	Do nothing	Low	Extremely high
Sce. 2		High	
Sce. 3		Extremely high	
Sce. 4	Riverbed widening	Low	
Sce. 5		High	
Sce. 6		Extremely high	

3.4 $m \cdot s^{-1}$ (2013).

The results shows that the maximum water surface elevation (Max WSE) of Sce. 3 is extremely higher than the power plant ground elevation (PPGE). After widening the riverbed,

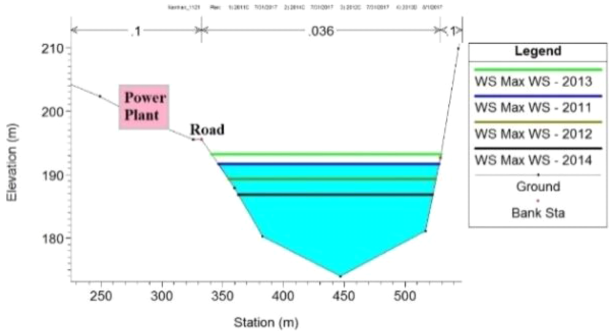

Fig. 8. Maximum surface water elevation from 2011 to 2014.

Max WSE Sce. 6 is slightly greater than the PPGE. The flood depths under most of scenarios are extremely high compared to the road elevation (RE) except Sce. 4 (Fig. 9). Although the water flow of Dong River is extremely high, the risk will be low if the flow of the upper Namhan River is low (Sce. 4). Other scenarios shows that the extremely high water flows in both upper reaches (i.e. upper Namhan and Dong River) can cause the flood. Therefore, the higher flow of the upper Namhan River affects the downstream reach more significantly than Dong River.

The flood depths under Sce. 1, Sce. 4 and Sce. 5 do not affect the power plant. Sce. 2 and Sce. 3 affect the power plant with the maximum depth are 0.43 m and 1.52 m above the PPGE respectively. Despite widening the riverbed, Sce. 6 still impacts on the PPGE with the maximum depth is 0.34

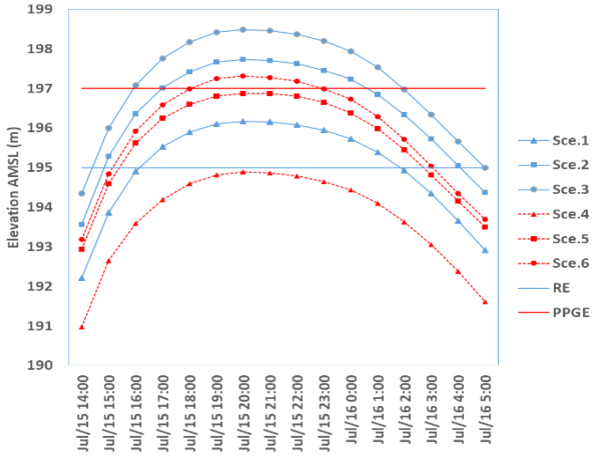

Fig. 9. Simulated water surface elevations following the future climate change scenarios.

m (Fig. 9 and Table 3).

In the comparison between Sce. 1 and Sce. 4, only flood depths under Sce. 1 affects the RE. Therefore, the riverbed widening strategy is highly effective for this case (low flow of the upper Namhan River). For the second case (high flow of the upper Namhan River), the widening strategy is useful for preventing the flood impact on the PPGE, with the maximum flood depth decreases from 0.43 m in Sce. 2 to 0.00 m in Sce. 5; however, it is not effective for the RE. The widening strategy may reduce the flood depths but may not be helpful for both PPGE and RE in the third case (extremely high flow of the upper Namhan River).

3.2 Velocities

A small part of lower Namhan River, from cross-section 43 to cross-section 40, was chosen to compare the velocities among the scenarios. It can be seen that the maximum velocities of the river will decrease if the riverbed is widened. The velocity under Sce. 4 is lower than Sce. 1; the velocity under Sce. 5 is lower than Sce. 2; and, velocity under Sce. 6 is lower than Sce. 3 (Fig. 10). The very high velocities cause river bank erosion, the riverbed widening strategy therefore help to reduce the risk of bank erosion.

4. CONCLUSIONS

In this research, the historical and topographical data are used for developing the one dimensional hydraulic model for predicting the water levels based on the climate change scenarios. The accuracy of the model is very reliable with the NS

Table 3. Inundation depths under six scenarios (m)

Scenario	On PPGE	On RE
Sce. 1	0.00	1.20
Sce. 2	0.43	2.43
Sce. 3	1.52	3.52
Sce. 4	0.00	0.00
Sce. 5	0.00	1.20
Sce. 6	0.34	2.34

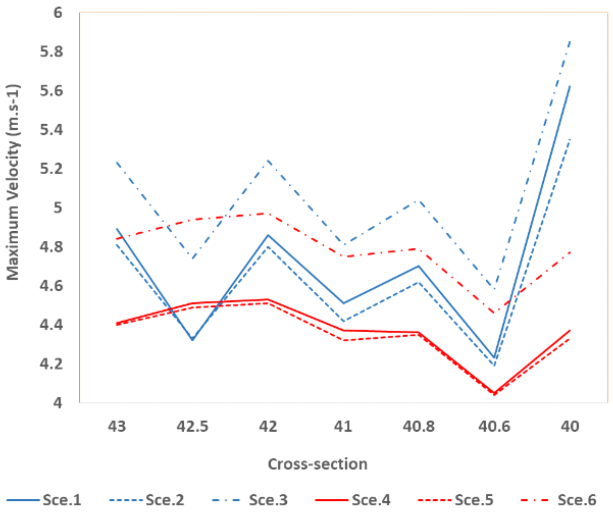

Fig. 10. Maximum velocities in the part of river near power plant.

values, are more than 0.9 through calibration and validation, result in the model can be applied for studying the climate change prediction.

The flood depths will decrease significantly if the riverbed is widened. The expected scenario is Sce. 4 and the most extreme flood event scenario is Sce. 3. The riverbed widening is an effective strategy for flood prevention for both road and power plant in the case that the water flow of Dong River is extremely high and the flow of the upper Namhan River is low. In case of high flow of the upper Namhan, the strategy is only effective for the power plant, and it is not effective for both power plant and road in case of the extremely high flow case. Besides, riverbed widening can help reduce the water velocities and therefore decrease the risk of bank erosion. Although the flow of Dong River is high, the risk will be not significant if the flow of the upper Namhan River is low under the widening strategy. Therefore, the impact of high flow of the upper Namhan River is more important than Dong River.

Although the results can help evaluate and predict the flood risk depending on future climate change scenarios, there remain some limitations. The riverbed elevations were just interpolated from the digital elevation model with the low resolution. In the further study, the two dimensional models with lateral structures should be developed. Moreover, the hydrological model with the relation between rainfall, basin and discharge

should be studied.

ACKNOWLEDGEMENT

This project is supported by the "R&D Center for reduction of Non-CO_2 Greenhouse gases (2016001690005)" funded by Korea Ministry of Environment (MOE) as "Global Top Environment R&D Program".

REFERENCES

Alegre P, Ferreira DM, Gomes, J. 2017. Verification of Saint-Venant equations solution based on the lax diffusive method for flow routing in natural channels. Brazilian J. Water Resour.

Anderson J, Bausch C. 2006. Climate change and natural disasters: Scientific evidence of a possible relation between recent natural disasters and climate change.

Bae DH, Jung IW, Lettenmaier DP. 2011. Hydrologic uncertainties in climate change from IPCC AR4 GCM simulations of the Chungju Basin, Korea. J Hydrol 401:90-105.

Bilskie MV, Hagen SC, Alizad K, Medeiros SC, Passeri DL, Needham HF, Cox A. 2016. Dynamic simulation and numerical analysis of hurricane storm surge under sea level rise with geomorphologic changes along the northern Gulf of Mexico. Earth's Futur. n/a-n/a.

Brunner G. 2010. HEC River Analysis System (HEC-RAS), http://www.hec.usace.army.mil/

Canestrelli A, Lanzoni S, Fagherazzi S. 2014. One-dimensional numerical modeling of the long-term morphodynamic evolution of a tidally-dominated estuary: The lower fly river (Papua New Guinea). Sediment Geol 301:107-119.

Chang H, Franczyk J, Kim C. 2009. What is responsible for increasing flood risks? The case of Gangwon Province, Korea. Nat Hazards 48:339-354.

Cheikh MB. 2015. Using of Hec-ras model for hydraulic analysis of a river with agricultural vocation: A case study of the Kayanga river basin, Senegal. American Journal of Water Resources 3(5):147-154.

Chow VT, Maidment DR, Mays LW. 1988. Applied hydrology. McGraw-Hill.

de Bruijn K, Buurman J, Mens M, Dahm R, Klijn F. 2017. Resilience in practice: Five principles to enable societies to cope with extreme weather events. Environ Sci Policy 70:21-30.

de Paes RP, Brandão JLB. 2013. Flood control in the Cuiab? River Basin, Brazil, with multipurpose reservoir operation. Water Resour Manag 27:3929-3944.

Easterling DR, Meehl GA, Parmesan C, Changnon SA, Karl TR, Mearns LO. 2000. Climate extremes: Observations, modelling, and impacts. Science 289:2068-2074.

Habert J, Ricci S, Le Pape E, Thual O, Piacentini A, Goutal N, Jonville G, Rochoux M. 2016. Reduction of the uncertainties in the water level-discharge relation of a 1D hydraulic model in the context of operational flood forecasting. J Hydrol 532:52-64.

Harmel RD, Smith PK, Migliaccio KW. 2010. Modifying goodness-of-fit indicators to incorporate both measurement and model uncertainty in model calibration and validation. Trans ASABE 53:55-63.

Jeong CS, Heo JH, Bae DH, Georgakakos KP. 2005. Utility of high-resolution climate model simulations for water resources prediction over the Korean peninsula: A sensitivity study. Hydrol Sci Journal-Journal Des Sci Hydrol 50:139-153.

Jonkman SN, Vrijling JK. 2008. Loss of life due to floods. J Flood Risk Manag 1:43-56.

Jung HS, Lim GH, Oh JH. 2001. Interpretation of the transient variations in the time series of precipitation amounts in Seoul, Korea. Part I: Diurnal variation. J Clim 14: 2989-3004.

Kim J, Choi J, Choi C, Park S. 2013. Impacts of changes in climate and land use/land cover under IPCC RCP scenarios on streamflow in the Hoeya River Basin, Korea. Sci Total Environ 452-453, 181-195.

Lotsari E, Aaltonen J, Veijalainen N, Alho P, Käyhkö J. 2014. Future fluvial erosion and sedimentation potential of cohesive sediments in a coastal river reach of SW Finland. Hydrol Process 28:6016-6037.

Meert P, Pereira F, Willems P. 2016. Computationally efficient modelling of tidal rivers using conceptual reservoir-type models. Environ Model Softw 77:19-31.

Mohleji S. 2011. Gaining from losses: Using disaster loss data as a tool for appraising natural disaster policy. Pro-

Quest Diss Theses.

Monirul Qader Mirza M. 2002. Global warming and changes in the probability of occurrence of floods in Bangladesh and implications. Glob Environ Chang 12:127-138.

Moriasi D, Arnold J. 2007. Model evaluation guidelines for systematic quantification of accuracy in watershed simulations. Transactions of the ASABE 50:885-900.

Na JI, Okada N, Fang L. 2012. Utilization of the Yonmen-kaigi system method for community building of a disaster damaged village in Korea. Conf Proc IEEE Int Conf Syst Man Cybern 3093-3098.

Nash JE, Sutcliffe JV. 1970. River flow forecasting through conceptual models. J Hydrol 10:282-290.

Paiva RCD, Collischonn W, Tucci CEM. 2011. Large scale hydrologic and hydrodynamic modeling using limited data and a GIS based approach. J Hydrol 406:170-181.

Panda RK, Pramanik N, Bala B. 2010. Simulation of river stage using artificial neural network and MIKE 11 hydrodynamic model. Comput Geosci 36:735-745.

Saleh F, Ducharne A, Flipo N, Oudin L, Ledoux E. 2013. Impact of river bed morphology on discharge and water levels simulated by a 1D Saint-Venant hydraulic model at regional scale. J Hydrol 476:169-177.

Savage JTS, Bates P, Freer J, Neal J, Aronica G. 2016. When does spatial resolution become spurious in probabilistic flood inundation predictions? Hydrol Process 30:2014-2032.

Wu T, Zheng Z, Ma W. 2015. Application of HEC-RAS in floating bridge calculation of the backwater height 205-208.

WWAP. 2009. The United Nations world water development report 3, Case study volume: Facing the challenges, World water.